ChemComm

RSC Publishing

COMMUNICATION

View Article Online
View Journal | View Issue

"Clickable" LNA/DNA probes for fluorescence sensing of nucleic acids and autoimmune antibodies†

Cite this: *Chem. Commun.*, 2013, **49**, 10751

Received 20th July 2013,
Accepted 19th September 2013

DOI: 10.1039/c3cc45507f

www.rsc.org/chemcomm

Anna S. Jørgensen, Pankaj Gupta, Jesper Wengel and I. Kira Astakhova*

Herein we describe fluorescent oligonucleotides prepared by click chemistry between novel alkyne-modified locked nucleic acid (LNA) strands and a series of fluorescent azides for homogeneous (all-in-solution) detection of nucleic acids and autoimmune antibodies.

Several autoimmune disorders are characterized by production of antibodies against single- and double-stranded DNA. If not diagnosed and treated early, the autoimmune conditions can lead to serious health deterioration and even mortality.[1] The sequence-specific autoimmune antibodies (autoantibodies) against single-stranded DNA have been thoroughly studied.[2] In turn, non-sequence-specific autoantibodies against double-stranded DNA, a hallmark of autoimmune conditions such as antiphospholipid syndrome and systemic lupus erythematosus (SLE), have not been studied in detail.[1]

Generally, monitoring interactions of nucleic acids by fluorescence is a convenient method in modern bioanalysis and can be performed under native conditions without additional equipment or procedures. Currently, fluorescent oligonucleotides containing bright cyanine and xanthene dyes are often applied in bioanalysis of nucleic acids[3] and proteins, including antibodies.[4] Furthermore, affinity-enhancing locked nucleic acids containing 2′-amino-LNA monomers with fluorescent polyaromatic hydrocarbons (PAHs) attached at the 2′-amino group provide high target binding affinity and selectivity, remarkable fluorescence quantum yields and brightness values.[5] Another appealing aspect of LNA/DNA probes is their high potential as aptamers in selective binding of diverse proteins.[6]

Herein, a new alkyne-LNA nucleotide **M¹** incorporated into synthetic oligonucleotides was used in copper(I)-catalyzed azide–alkyne cycloaddition (CuAAC or "click")[7] reactions with xanthene, cyanine and PAH azides **5–8** (Scheme 1). We describe preparation and the bioanalytical potential of the resulting LNA/DNA probes in fluorescence homogeneous sensing of nucleic acids and autoantibodies against double-stranded DNA, as well as structural aspects of the interactions clarified by the developed fluorescence assay.

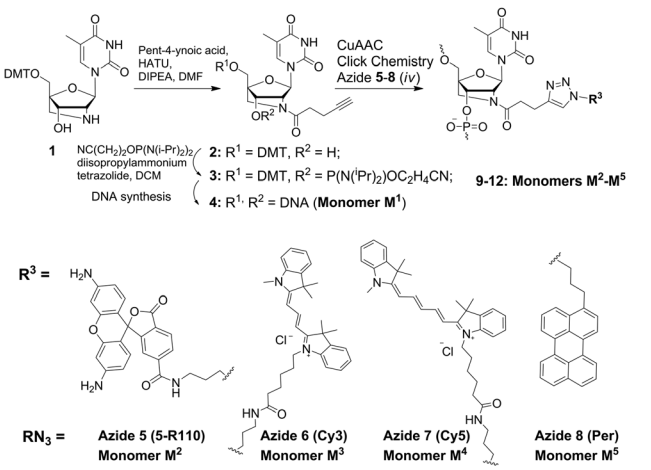

Scheme 1 Synthesis of alkyne-LNA monomer **M¹** and incorporation of monomers **M¹–M⁵** into synthetic oligonucleotides.

Previously, satisfactory biosensing properties of fluorescent probes labelled at the 2′-position of uridine by CuAAC reactions were demonstrated.[8] In the present study we designed alkyne-LNA monomer **M¹** which combines the unique bicyclic structure of 2′-amino-LNA[5] with a terminal alkyne group, allowing post-synthetic attachment of different tags by click chemistry.

Monomer **M¹** was incorporated into oligonucleotides using the phosphoramidite building block **3** which was prepared starting from the corresponding 2′-amino-5′-*O*-dimethoxytrityl protected LNA nucleoside **1** in two steps with 52% overall yield. Subsequent automated DNA synthesis furnished modified 21-mer oligonucleotides similar to those previously used in studies of 2′-alkyne-uridine (Scheme 1 and Table 1).[10] After purification and characterization by ion-exchange (IE) HPLC and MALDI-MS (ESI†), **ON1–ON4** were subjected to CuAAC reactions with fluorescent azides of three important classes: xanthene 5-R110 (**5**), cyanines Cy3 and Cy5 (**6** and **7**, respectively), and PAH perylene **8** (Table S1, ESI†).

Nucleic Acid Center, Department of Physics, Chemistry and Pharmacy, University of Southern Denmark, DK-5230 Odense M, Denmark. E-mail: ias@sdu.dk; Fax: +45 6615 8780; Tel: +45 6550 2510

† Electronic supplementary information (ESI) available: Synthesis of monomer **M¹**, oligonucleotide synthesis and purification, click chemistry, NMR, MALDI-MS, IE HPLC and T_m data; fluorescence diagnostic assays and representative emission spectra, quantum yields, and molecular modeling. See DOI: 10.1039/c3cc45507f

Table 1 Sequences of oligodeoxyribonucleotides (ONs) and thermal denaturation temperatures of the duplexes prepared in this study[a]

		$T_m/\Delta T_m$ (°C)	
		Target	
ON	Sequence, 5′ → 3′	DNA	RNA
DNA^{ref}	TGCACTCTATGTCTGTATCAT	59.0	60.5
ON1	TGCACTCTATG**M^1**CTGTATCAT	62.0/+3.0	65.0/+4.5
ON2	TGCACT CTA**M^1**GTC**M^1**GTAT CAT	63.5/+4.5	69.0/+8.5
ON3	TGCAC**M^1**CTATGTCTGTA**M^1**CAT	63.0/+4.0	68.0/+7.5
ON4	TGCAC**M^1**CTATG**M^1**CTGTA**M^1**CAT	65.0/+6.0	71.0/+10.5
ON5	TGCACTCTATG**M^2**CTGTATCAT	59.0/0.0	62.0/+1.5
ON6	TGCACT CTA**M^2**GTC**M^2**GTAT CAT	60.0/+1.0	66.0/+5.5
ON7	TGCAC**M^2**CTATGTCTGTA**M^2**CAT	58.0/−1.0	64.0/+3.5
ON8	TGCAC**M^2**CTATG**M^2**CTGTA**M^2**CAT	58.0/−1.0	66.0/+5.5
ON9	TGCACTCTATG**M^3**CTGTATCAT	62.0/+3.0	63.0/+2.5
ON10	TGCACT CTA**M^3**GTC**M^3**GTAT CAT	63.0/+4.0	66.0/+5.5
ON11	TGCAC**M^3**CTATGTCTGTA**M^3**CAT	63.0/+4.0	65.0/+4.5
ON12	TGCAC**M^3**CTATG**M^3**CTGTA**M^3**CAT	65.0/+6.0	66.5/+6.0
ON13	TGCACTCTATG**M^4**CTGTATCAT	62.0/+3.0	63.0/+2.5
ON14	TGCACT CTA**M^4**GTC**M^4**GTAT CAT	64.0/+5.0	65.0/+4.5
ON15	TGCAC**M^4**CTATGTCTGTA**M^4**CAT	63.0/+4.0	64.5/+3.5
ON16	TGCAC**M^4**CTATG**M^4**CTGTA**M^4**CAT	65.0/+6.0	65.5/+5.0
ON17	TGCACTCTATG**M^5**CTGTATCAT	66.0/+7.0	65.0/+4.5
ON18	TGCACT CTA**M^5**GTC**M^5**GTAT CAT	70.0/+11.0	60.0/−0.5
ON19	TGCAC**M^5**CTATGTCTGTA**M^5**CAT	67.0/+8.0	67.0/+6.5
ON20	TGCAC**M^5**CTATG**M^5**CTGTA**M^5**CAT	72.0/+13.0	70.0/+9.5

[a] Thermal denaturation temperatures T_m (°C)/change in T_m relative to the corresponding unmodified duplex, ΔT_m (°C) (ESI).

Conditions of the click chemistry were adjusted for each azide, taking into account the high hydrophobicity of the cyanine and perylene dyes, giving 62–81% yields of the products in ≥95% purity as determined by IE HPLC (Table S2, ESI†).

Binding affinity of **ON5–ON20** to complementary and mismatched DNA/RNA targets was evaluated in a medium salt phosphate buffer ([Na^+] = 110 mM, pH 7.0) by thermal denaturation (T_m) measurements monitoring absorbance at 260 nm and at the characteristic fluorophores' wavelength (Tables S3–S5, ESI†). First, the resulting T_m values were similar at both wavelengths suggesting high sensitivity of the dyes to hybridization. Second, affinity enhancing LNA monomers resulted in high T_m values of the duplexes with complementary DNA/RNA suggesting that the fluorophores are tolerated within the double strands as described earlier for other fluorophores.[8] Further, especially high target binding was displayed by the probes having **M^5** (ΔT_m up to +13 °C for three incorporations), most likely provided by additional interactions involving the attached perylene groups. Third, thermal denaturation values for the selected probes **ON7** and **ON19** were decreased by 8–18 °C in the presence of a single mismatch in target DNA/RNA, confirming high binding selectivity for the examined probes (Table S4, ESI†; the probes were selected based on their attractive fluorescence properties as potential biosensors described below).

Notably, hybridization resulted in hypsochromic shift of absorbance maxima by the monomer **M^2** ($\Delta\lambda^{abs}_{max}$ 7–9 nm), confirming placement of the xanthene within the minor groove of the duplexes.[8] In turn, **M^3**–**M^5** showed minor changes in absorbance peaks upon binding DNA/RNA ($\Delta\lambda^{abs}_{max}$ 1–3 nm), although in the case of the cyanine monomers **M^3**–**M^4** the ratio between two visible absorbance bands (RI\II) increased upon hybridization. According to the literature[9] this indicates reduced dye interactions upon hybridization

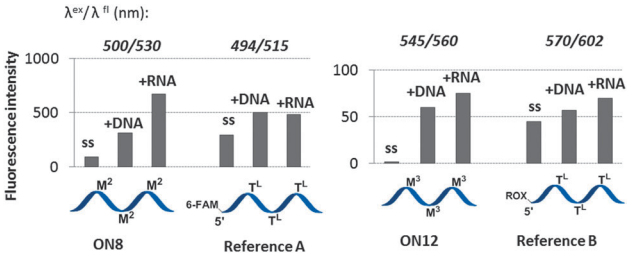

Fig. 1 Representative fluorescence intensities of the probes (ss) and duplexes compared to 5′-labelled LNA/DNA references. Spectra were obtained in a medium salt buffer at 19 °C using 1.0 μM oligonucleotides. Reference A: 5′-(6-FAM)-d(TGC AC$\underline{T}^L$ CTA TG $\underline{T}^L$ CTG TA$\underline{T}^L$ CAT)-3′; reference B: 5′-ROX-d(TGC AC$\underline{T}^L$ CTA TG $\underline{T}^L$ CTG TA$\underline{T}^L$ CAT)-3′. T^L = LNA-T nucleotide.

and their aggregation within single-stranded probes (Fig. S5, ESI;† *e.g.* RI\II 1.0 and 2.3 for **ON16** and **ON16**:RNA, respectively).

Steady-state fluorescence emission spectra of **ON5–ON20** and their duplexes with DNA/RNA targets were recorded in a medium salt buffer at 19 °C. In order to evaluate the effect of internal attachment of the fluorophores on fluorescence properties of the probes, their fluorescence intensities were compared to those of 5′-labelled LNA/DNA references (Fig. 1; Table S1, ESI†). As confirmed by fluorescence spectra, large hydrophobic dyes **M^2**–**M^4** aggregated in a highly polar environment of the single-stranded probes, which resulted in quenched fluorescence (Table S6, ESI;† fluorescence quantum yields Φ_F 0.01–0.16).[8,9] Similarly, fluorescence of the duplexes possessing internally incorporated cyanine monomers **M^3** and **M^4** was low (Φ_F 0.01–0.11), most likely due to active interactions of the dyes and nucleic acids.[8] In contrast, fluorescence intensity of single-stranded probes and duplexes containing monomer **M^5** was extraordinarily high (Φ_F 0.54–1.00 and fluorescence brightness (FB) values up to 80). Efficient sensing of hybridization accompanied by high Φ_F and FB values was displayed exclusively by the probes **ON7** and **ON8** having double and triple incorporation of the monomer **M^2**, respectively (Fig. 2; ESI†). Upon binding complementary targets by **ON7** and **ON8**, up to 7.8-fold light-up of fluorescence was observed at λ^{fl}_{max} 530 nm, accompanied by Φ_F 0.22–0.45 and FB values up to 77 of the corresponding duplexes. Being compared to commercially available 5′-modified LNA/DNA references (Fig. 2) and other fluorescent probes,[3,8,9] the probes prepared herein generally display improved binding affinity, sensing of hybridization, fluorescence quantum yield

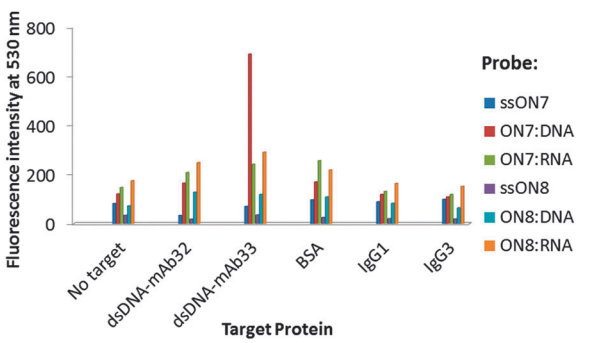

Fig. 2 Fluorescence detection of monoclonal autoantibodies (ESI†).

and brightness values, which are important properties for their application in various bioanalytical assays. Finally, fluorescence intensities of duplexes formed by **ON7** and **ON19** decreased 1.9–9.9 times in the presence of single-base mismatches in target DNA/RNA (Table S4, ESI†). Decreased emission in the presence of a mismatch is most likely caused by high sensitivity of the fluorescence of the internally incorporated monomers $\mathbf{M^2}$ and $\mathbf{M^5}$ to the local microenvironment within the biomolecules.[8]

An important advantage of synthetic oligonucleotides within molecular diagnostics of proteins (so-called aptasensing approach) and immunoimaging techniques is their high specificity in binding a target.[10] To assess the potential of the novel probes in diagnostics of clinically important proteins, fluorescence homogenous detection of human autoantibodies against double-stranded DNA was performed. Single-stranded **ON7–ON8** and their duplexes with complementary DNA/RNA were incubated with commercially available human monoclonal autoantibodies dsDNA-mAb32 and dsDNA-mAb33, which were recently studied by surface plasmon resonance (SPR).[10] The subtypes of the monoclonal antibodies were IgG1 (dsDNA-mAb33) and IgG3 (dsDNA-mAb32), and both antibodies have been used as serological parameters in diagnostics of SLE.[11]

Incubation was then performed in a medium salt phosphate buffer at 37 °C for 1 h followed by analysis after 2 h at 19 °C (ESI†). In order to evaluate the probes' specificity bovine serum albumin (BSA) and non-specific isotype antibodies IgG1 and IgG3 were used as references.[12] Unlike single-stranded **ON7** and other examined complexes, **ON7**:DNA showed 5.7-fold increase of fluorescence at 530 nm when binding dsDNA-mAb33, and 4.2-fold greater fluorescence than in the presence of dsDNA-mAb32, BSA or IgG controls (Fig. 2). Previously SPR studies indicated weaker binding for dsDNA-mAb33 compared to dsDNA-mAb32 by a 24 bp DNA duplex ($(k_d)_{obs} \sim 6.5 \times 10^{-3}$ s^{-1} and 0.5×10^{-3} s^{-1}, respectively).[10] Thus, the binding pattern of **ON7**:DNA implies that chemical modification might change binding properties of nucleic acids to target proteins. In contrast to **ON7**:RNA and triply modified **ON8**:DNA/RNA, little to no fluorescence signal of interaction with BSA or non-specific isotype IgGs was observed for **ON7**:DNA, confirming high binding selectivity for the latter complex (Table S7, ESI†). According to our molecular models, triple incorporation of the xanthene dyes ($\mathbf{M^2}$) results in high surface hydrophobicity of the duplexes, which may account for their non-specific binding to BSA (ESI;† Fig. S7a). In turn, effective recognition of dsDNA-mAb33 is provided by steric and chemical complementarity of the unmodified internal region of **ON7**:DNA and the variable region of the autoantibody's heavy chain, accompanied by effective hydrogen bonding (Fig. S7b, ESI,† compared to c and d). We speculate that similarly to hybridization described above, target binding results in positioning of the xanthenes in a less polar environment compared to the initial nucleic acid complex resulting in an increased fluorescence.

Finally, the limit of target detection (LOD) for **ON7**:DNA was determined to be below 4.6 μg mL^{-1} of dsDNA-mAb33 (Fig. S8, ESI†). This is comparable with currently applied enzyme-linked immunosorbent assay (ELISA), immunofluorescence tests (LOD approx. 1–2 μg mL^{-1}),[1] and other fluorescent aptasensors.[13] Notably, being compared to voltage current and electrochemical methods, homogeneous detection is robust, rapid and does not affect interacting surfaces of the biomolecules which can be detected without the need for additional steps and reagents.[13,14]

In conclusion, the click approach presented here efficiently yields probes with various dyes attached internally at the 2′-amino-position of 2′-amino-LNA monomers. This approach provides a reliable foundation for simple and efficient preparation of a library of fluorescent probes, screening and identification of several bright oligonucleotides with high target binding affinity and specificity. As demonstrated by our initial studies, potential applications of these probes include a wide range of fluorescence assays including, but not limited to, live-cell nucleic acid imaging, aptasensing and nucleic acid diagnostics. Moreover, the 2′-*N*-alkynyl group in the LNA/DNA strands is available for the attachment of other tags such as carbohydrates, lipids, cofactors and cell-penetrating peptides. In this context we believe that "clickable" LNA/DNA probes offer appealing opportunities for developing efficient tools for biosensing, pharmacological or nano-production purposes.

The authors would like to acknowledge financial support from The Sapere Aude programme of The Danish Council for Independent Research, THE VILLUM FOUNDATION and The European Research Council under the European Union's Seventh Framework Programme (FP7/2007-2013)/ERC Grant agreement No. 268776.

Notes and references

1 B. Giannakopoulos, F. Passam, Y. Ioannou and S. A. Krilis, *Blood*, 2009, **113**, 985.
2 P. C. Ackroyd, J. Cleary and G. D. Glick, *Biochemistry*, 2001, **40**, 2911.
3 M. D. Blower, E. Feric, K. Weis and R. Heald, *J. Cell Biol.*, 2007, **179**, 1365.
4 S. C. B. Gopinath, K. Awazu and M. Fujimaki, *Sensors*, 2012, **12**, 2136.
5 I. V. Astakhova, D. Lindegaard, A. D. Malakhov, V. A. Korshun and J. Wengel, *Chem. Commun.*, 2010, **46**, 8362; M. E. Østergaard and P. J. Hrdlicka, *Chem. Soc. Rev.*, 2011, **40**, 5771.
6 K. K. Karlsen and J. Wengel, *Nucleic Acid Ther.*, 2012, **22**, 366.
7 V. C. Spiteri and J. E. Moses, *Angew. Chem., Int. Ed.*, 2010, **49**, 31.
8 I. K. Astakhova and J. Wengel, *Chem.–Eur. J.*, 2013, **19**, 1112; M. M. Rubner, C. Holzhauser, P. R. Bohländer and H.-A. Wagenknecht, *Chem.–Eur. J.*, 2012, **18**, 1299; S. P. Sau and P. J. Hrdlicka, *J. Org. Chem.*, 2012, **77**, 5; A. H. El-Sagheer and T. Brown, *Acc. Chem. Res.*, 2012, **45**, 1258.
9 F. Würthner, T. E. Kaiser and C. R. Saha-Möller, *Angew. Chem., Int. Ed.*, 2011, **50**, 3376.
10 A. Buhl, S. Page, N. H. H. Heegaard, P. von Landenberg and P. B. Luppa, *Biosens. Bioelectron.*, 2009, **25**, 198.
11 T. H. Winkler, S. Jahn and J. R. Kalden, *Clin. Exp. Immunol.*, 1991, **85**, 379; dsDNA-mAb32 and dsDNA-mAb33 correspond to clones 32.B9 and 33.H11, respectively.
12 Y. Zhanga and X. Sun, *Chem. Commun.*, 2011, **47**, 3927.
13 C.-H. Leung, D. S.-H. Chan, H.-Z. He, Z. Cheng, H. Yang and D.-L. Ma, *Nucleic Acids Res.*, 2012, **40**, 941.
14 L. Wang, Q. Zheng, Q. Zhang, H. Xu, J. Tong, C. Zhu and Y. Wan, *Oncol. Lett.*, 2012, **4**, 935; S. Xie, Y. Chai, R. Yuan, L. Bai, Y. Yuan and Y. Wang, *Anal. Chim. Acta*, 2012, **755**, 46.